

Testing the 2020 European Seismic Hazard Model (ESHM20) against observations from Romania

1 Elena F. Manea^{1,2}, Laurentiu Danciu³, Carmen O. Cioflan¹, Dragos Toma-Danila¹, Matthew C.
2 Gerstenberger²

3 ¹ National Institute for Earth Physics, Măgurele, 077125, Ilfov, Romania

4 ² GNS Science, PO Box 30-368, Lower Hutt, New Zealand

5 ³ ETH Zurich, Seismology and Geodynamics, Sonneggstrasse 5, 8092 Zurich, Switzerland

6

7 *Correspondence to:* Elena F. Manea (flory.manea88@gmail.com); Laurentiu Danciu (laurentiu.danciu@sed.ethz.ch)

Abstract. Evaluating the performance of probabilistic seismic hazard models against recorded data and their potential to forecast future earthquake's ground shaking is an emerging research topic. In this study, we evaluate and test the results of the recently released European Seismic Hazard Model (ESHM20; Danciu et al., 2021, Danciu et al 2024) against observations for several cities in Romania. The dataset consists of ground shaking recordings and macroseismic observations, which extend the observational time-period to a few hundred years. The full distribution of the hazard curves, depicting the epistemic uncertainties of the hazard at the given location was considered and the testing was done for peak ground acceleration (PGA) values, 0.1g and 0.2g.

The results show consistency between the ESHM20 and the ground motion observations for the cities located near the Vrancea intermediate-depth source (VRI) for both selected PGA levels. ESHM20's estimated values appear to be over the VRI recorded ground motions along the Carpathian Mountain Range and below those at the far-field locations outside the Carpathians, yet inside the expected model variability. Some of these differences might be attributed to the uncertainties in data conversion, local site effects, or differences in the attenuation patterns of the ground motion models. Our analysis suggests that the observed exceedance rates for the selected PGA levels are consistent with ESHM20 estimates, but these results must be interpreted with caution given the limited time and spatial coverage of the observations.

9 Probabilistic seismic hazard analysis (PSHA) is an important framework in seismology and earthquake engineering, widely
10 used worldwide to quantify the uncertainty inherent in both the occurrence and effects of earthquakes. PSHA underpins a wide
11 range of applications, from the development of modern seismic design building codes to seismic risk assessments. It also
12 informs various public policy and risk management strategies aimed at mitigating the impacts of seismic events.

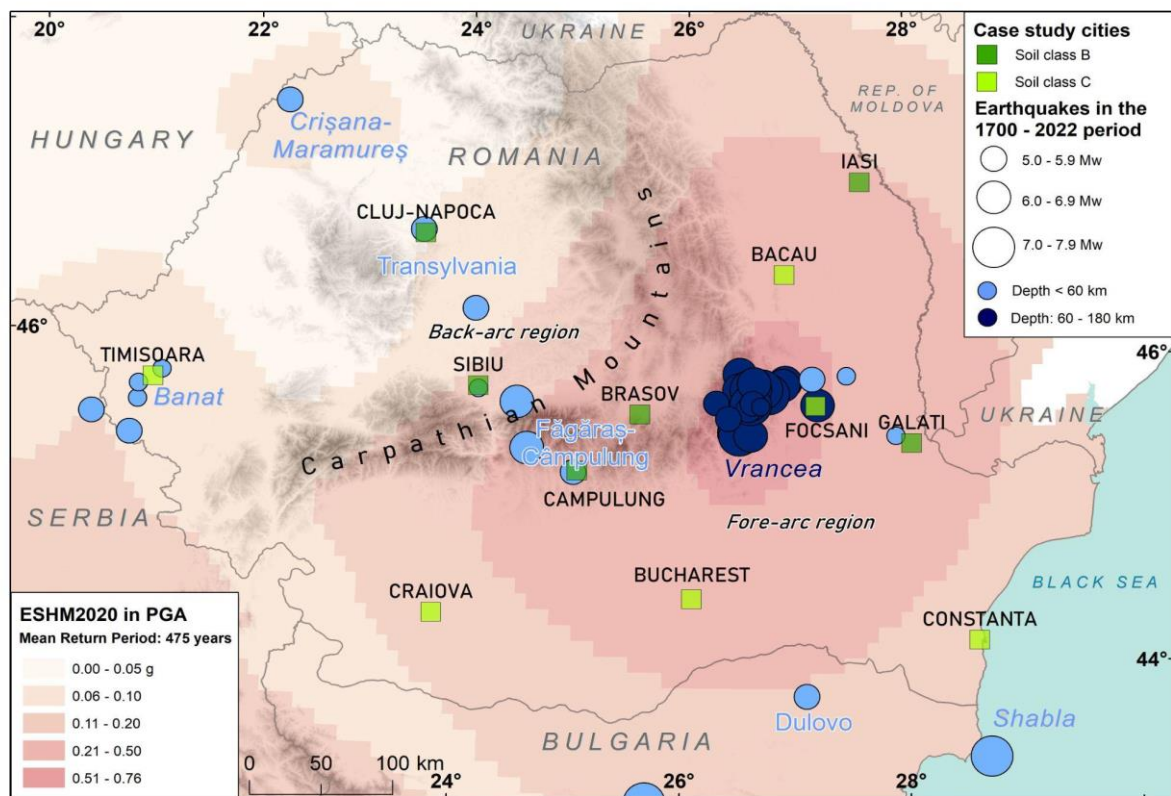
13 Despite its widespread adoption, testing the PSHA results is not straightforward. The sporadic nature of earthquakes, coupled
14 with low rate of occurrence, or low probabilities and high consequences events, makes the empirical validation of PSHA
15 models and results a task that would typically require observations spanning multiple human lifetimes (e.g. Vanneste et al.,
16 2018; Gerstenberger et al., 2020; Allen et al., 2023). For instance, in regions like France or Germany, where the installation of
17 accelerometric stations began in the mid-1990s, the availability of the instrumental records is limited to a short temporal
18 window. Even in more seismically active regions like Italy, Turkey or Greece, subject to more frequent damaging events,
19 validating probabilistic hazard models is challenging for the same reasons. In recent years, several procedures have emerged
20 aimed at testing seismic hazard estimates against past observations (e.g., Hanks et al., 2012; Marzocchi and Jordan, 2018).
21 These procedures are typically performed at short (e.g., Stirling and Gerstenberger, 2010; Tasan et al., 2014; Mousavi and
22 Beroza, 2016; Mak and Schorlemmer, 2016; Iervolino et al., 2023; Stirling et al., 2023) or long return periods (e.g., Rey et al.,
23 2018; Salditch et al., 2020; Meletti et al., 2021), depending on the aim of the application.

24 The current study aims to compare the recently released European Seismic Hazard Model (ESHM20; Danciu et al., 2021,
25 Danciu et al 2024) results against instrumental recordings and detailed macroseismic observations specific to Romania. This
26 region offers a distinctive seismo-tectonic landscape, dominated by the Vrancea intermediate-depth seismic source (VRI). The
27 VRI has a concentrated nest of seismicity at depths between 60 and 200 km, which is associated with the current dehydration
28 of an oceanic subducted plate, as noted by Ferrand and Manea (2021) and Craiu et al. (2022). Macroseismic intensities maxima
29 of strong VRI events are often observed/reported outside of the epicentral area: values of IX+ for 1940 event with the moment
30 magnitude $M_w=7.7$, and VIII+ (MSK-64 scale) for the 1977 event with $M_w=7.4$ (e.g. Kronrod et al., 2013).

31 The largest intensity values are found outside of the Carpathian belt, where a substantial number of sedimentary structures are
32 located (Marmureanu et al., 2016a; 2017; Manea et al., 2019). Beside this, the source properties imprint an asymmetric shape
33 to the macroseismic field, elongating it in the NE-SW direction (Marmureanu et al., 2016b). In contrast, strong back-arc
34 attenuation features are recorded within the Carpathian region and prescribe the current pattern of the macroseismic fields (e.g.
35 Vacareanu et al., 2015; Manea et al., 2022). The VRI impact extends beyond the national borders and significant damage has
36 been reported in neighbouring countries, with observed intensities of VII-VIII at more than 250 km epicentral distances during
37 the 7.7Mw 1940 event (Cioflan et al., 2016).

38 Furthermore, while the shallow crustal seismic activity in Romania is not as frequent as the one at intermediate depths in the
39 Vrancea region, it still poses a significant contribution to the regional seismic hazard (Marmureanu et al., 2016a). The main
40 seismic sources for such events are located along the Carpathian Mountains, particularly in the Făgăraș-Câmpulung zone, as

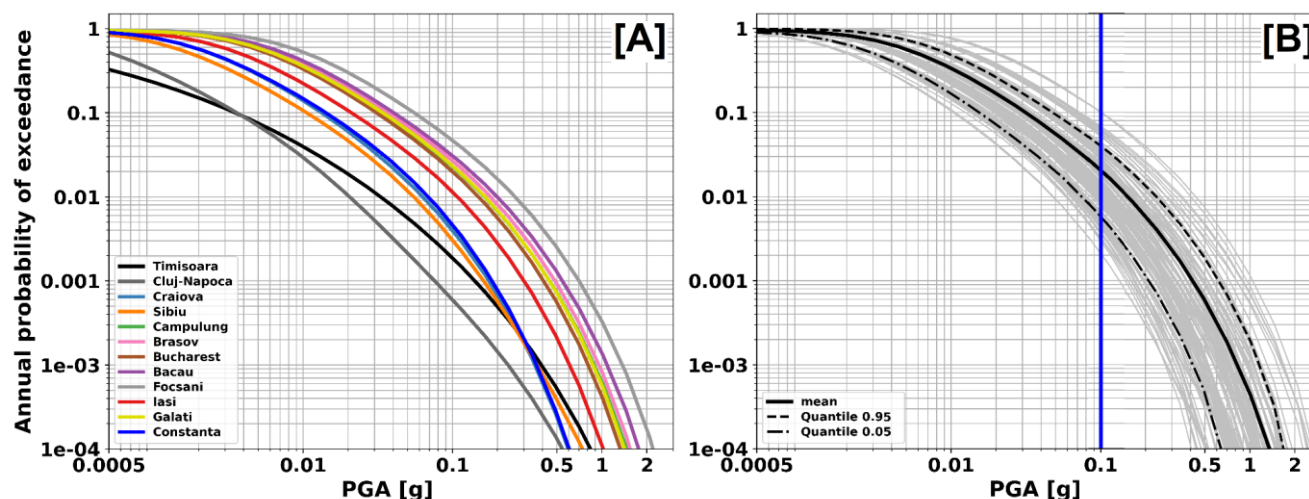
41 well as in the foreland regions of southwestern Romania, including Banat and Danubius, and extending northwest to Crisana-
 42 Maramures. Despite the lower rate of crustal activity in these areas compared to the Vrancea region, historical accounts and
 43 pre-instrumental catalogues document significant earthquakes with magnitudes $M_w \geq 5$ and epicentral intensities $I_0 \geq VI$ MSK
 44 scale (e.g., Radu, 1979; Oncescu et al., 1999). Thus, in this study, we consider intensity data spanning over three centuries
 45 from twelve important cities in Romania (see their locations in *Figure 1*). These urban areas are selected for their significant
 46 population and different exposure to seismic hazard levels. The present study begins with an overview of the ESHM20 and its
 47 specific relevance to Romania. It will then discuss the main components of the model and the results relevant at the regional
 48 level. The next section describes the main data, the curation and conversion procedure, which includes how historical
 49 macroseismic data were collected and converted into peak ground acceleration (PGA) values for different Romanian cities.
 50 Subsequently, a summary of the statistical testing process will be given, detailing the approaches taken to contrast the recorded
 51 seismic activity with the ESHM20 estimates. Next, the main outcomes of the statistical testing at two reference values for PGA
 52 - 0.1 and 0.2 g, are illustrated and interpreted, followed up by discussion and conclusions of our findings.



53
 54 **Figure 1: Location of the selected twelve cities and the post-1700 earthquakes (according to the Unified Earthquake Catalogues of**
 55 **the European Seismic Hazard Model 2020 - ESHM20; Danciu et al., 2021) used in this study. Only events with moment magnitude**
 56 **$M_w \geq 5$, for which at least one macroseismic intensity exceeding VI MSK-64 is recorded at the selected locations, were considered.**
 57 **The background is the ESHM20's ground shaking map in terms of peak ground acceleration (PGA) for a return period of 475 years.**

59 The 2020 European Seismic Hazard Model (ESHM20, Danciu et al 2021, 2022) is the latest revision and update of the seismic
60 hazard assessment for the Euro-Mediterranean region. ESHM20 is constructed using harmonised datasets that include
61 information on ground motion, earthquake catalogues, active faults, and tectonic data across different borders. The ground
62 shaking hazard in the region is estimated by combining a complex seismogenic source model, which includes distributed
63 seismicity, active faults, and subduction sources, with regionally scaled backbone ground motion models (Weatherill et al.,
64 2023). More specifically, the seismogenic source model consists of two branches of sources: the area source models and a
65 hybrid combination of active faults and background smoothed seismicity. In Romania, due to the lack of available data on
66 active faults, the seismogenic source model is based on an area source model and a smoothed seismicity with an adaptive
67 kernel. Furthermore, the seismogenic sources depicting the nested seismicity with depth in the Vrancea region are also
68 considered and modelled with a set of uniform area source zones located between 70 to 150 km depth. The ground motion
69 characteristic models for Romania are scaled based on regional factors to capture the ground shaking characteristics of both
70 the active shallow crust and non-subduction deep seismicity. These models are described by Weatherill et al., (2020, 2023). A
71 complex logic tree was developed to address the spatial and temporal variability in the earthquake rate forecast as well as the
72 regional backbone ground motion models. The computation was performed using OpenQuake (Pagani et al 2014) and the full
73 logic tree was sampled to obtain the distribution of the hazard results. For this analysis, we selected twelve major cities in
74 Romania, as illustrated in *Figure 1*, where we superimposed the ESHM20's ground shaking map in terms of peak ground
75 acceleration (PGA) for a return period of 475 years. Also, the relevant earthquakes with moment magnitude, $M_w \geq 5$ at which
76 at least one macroseismic intensity exceeding VI MSK-64 is recorded at the selected locations, are also plotted in the same
77 map. The highest PGA mean value is observed in the proximity of the Vrancea source, a region of high seismicity as indicated
78 also by the density of the seismic events (*Figure 1*). The pattern of PGA values follows the Carpathian Arc, with values
79 decreasing in the backarc towards the north-western part of the region. The range of PGA values is rather large, spanning from
80 0.15g in Cluj to 0.9 g observed for Focşani. The ESHM20's hazard curves for the mean PGA values at the selected cities in
81 Romania are presented in *Figure 2A* and show that the decay of the hazard curves is different, with a fast decay indicating
82 lower hazard and vice-versa. A significant spreading of the mean hazard curves is present between the locations outside and
83 within the Carpathian arc, following the same pattern as the 475 year mean ESHM20's ground shaking map (*Figure 2A*). The
84 highest annual probability of exceedances (APEs) is seen at locations in the proximity of the Vrancea source, which dominates
85 the hazard at all the return periods, while the lower values are observed at cities located in the far-field extent of this region,

86 where low-recurrence shallow seismicity is present. The full distribution of hazard curves for 10000 random sampled hazard
 87 curves along the ESHM20 logic tree for Bucharest is shown in *Figure 2B* together with the mean and the 5 and 95 percentiles
 88 At this location, the variability of the hazard curves presents a narrow range and depict the combined uncertainties of mainly
 89 the Vrancea source and ground motion (Danciu et al., 2024). Finally, we used the full distribution of the ESHM20 hazard
 90 curves to retrieve the statistical testing input, as described in the testing procedure section.
 91



92
 93 **Figure 2:** [A] The ESHM20’s annual probability of exceedance as a function of PGA (so called hazard curves) at the selected cities
 94 in Romania. [B] Full distribution of hazard curves for 10,000 samplings extracted across all the ESHM20 hazard branches for
 95 Bucharest city. The mean hazard is presented as a continuous black line, while the dashed ones represent the 5 and 95 percentiles.

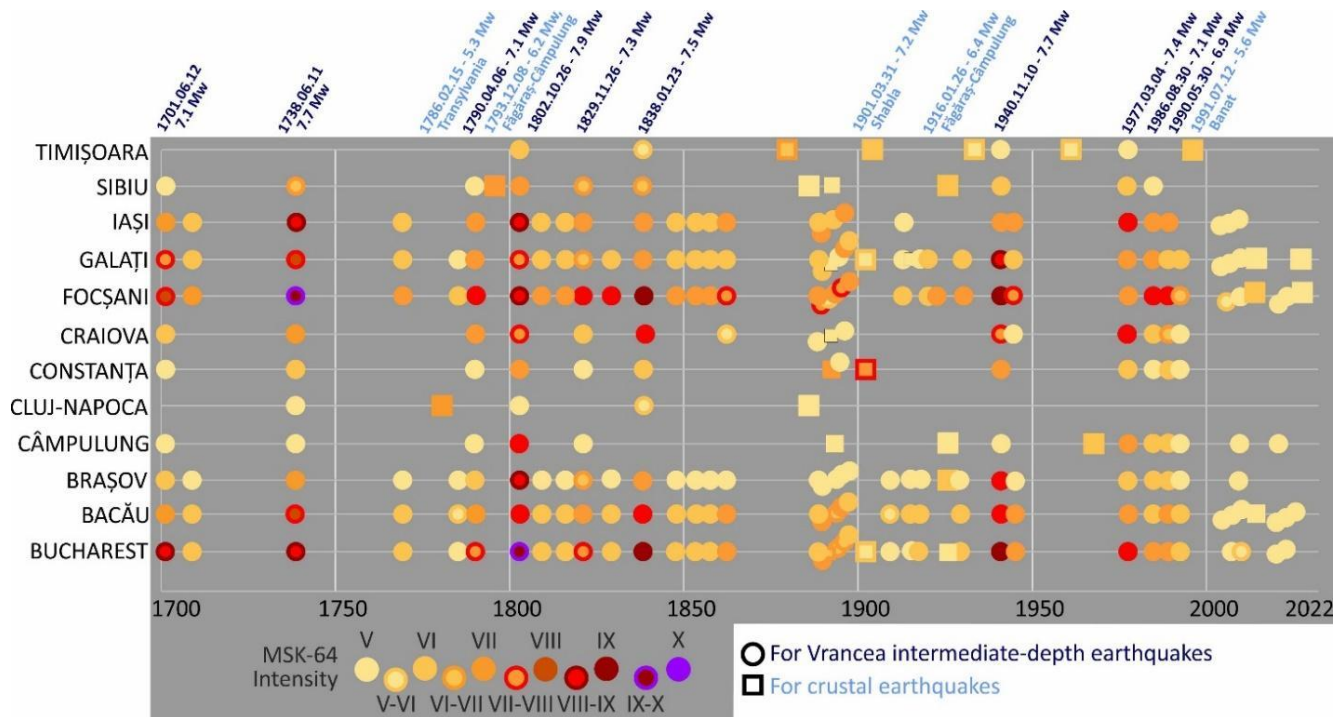
96
 97 **3 Available Data and Conversion**

98 Macroseismic intensity observations recorded over several hundreds of years (starting with 1700) at the main cities across
 99 Romania are used to test ESHM20’s results. The selected cities are among the most highly populated urban areas across
 100 Romania and are well-distributed with respect to the various seismic hazard levels and source characteristics shown by the
 101 ESHM20’s PGA hazard map for the 475 year return period (see *Figure 1*). It is noteworthy that these observations were
 102 collected within this study and were not directly used in the derivation of the ground motion component of the ESHM20,
 103 securing their independence for statistical testing. Intensity data points (IDP) were acquired from multiple available sources:
 104 Atanasiu (1961), Constantin et al. (2011, 2013, 2016, 2023), Kronrod et al. (2013), Marmureanu et al. (2018), Rogozea (2014;
 105 2016) and Shebalin et al. (1974). Beside compiling original information (i.e., intensity values), most of these studies are also
 106 providing new evaluations at locations where new macroseismic information became available. Note that, while IDPs of the

107 XVII-XVIII centuries had been evaluated from scarce information, the ones related with strong Vrancea earthquakes of the
108 20th century were collected through wide national campaigns (see details in Kronrod et al., 2013, Constantin et al., 2016).
109 Several IDPs of our initial dataset have a very local character as they strictly reflect the effects of strong intermediate-depth
110 earthquakes on specific buildings existing at the respective time (e.g. churches, monasteries; Marmureanu et al., 2018). Where
111 available, such site-specific intensity estimations are averaged with macroseismic data from other authors and various sources
112 (especially isoseismal maps). Additionally, maps published before 2000 have been checked against the information available
113 in the European Archive of Historical Earthquake Data platform (AHEAD; Rovida et al., 2020) which also helped us to fill in
114 the data gaps for some cities. If an IDP was not available at the specific location, a natural neighbour interpolation scheme
115 (Sibson, 1981) was used to extract it from georeferenced isoseismal maps selected from the above-mentioned sources. Some
116 of the collected IDPs were reported in the Rossi-Forel intensity scale (e.g., 7.1 Mw 1908 VRI earthquake) and were
117 homogenised to MSK-64 using the conversions proposed by Musson et al. (2010). Thus, we also treat MMI and EMS-98
118 intensity values as equivalent to MSK-64 ones. The MSK-64 is preferred as the VRI's intensity to ground motion conversion
119 equations (IGMCEs) were developed using this intensity scale for Romania.

120 From this collected dataset, we considered only IDP data from events with $M_w \geq 6$ for VRI and $M_w \geq 5$ for shallow seismicity
121 (see their locations in *Figure 1*) and with a minimum observed epicentral intensity I_0 of VII MSK-64, which corresponds to a
122 PGA value of 112 cm/s^2 for VRI (e.g. Ardeleanu et al., 2020) and/or 154 cm/s^2 (Caprio et al., 2015) for shallow seismicity.
123 The testing dataset at the twelve major cities contains 199 IDPs recorded from 58 earthquakes (see *Figure 1*), from which 39
124 are located in the VRI region. For each city, the time window of data completeness (Table 1) is visually evaluated based on
125 IDPs higher or equal to V (see Figure 3) from events considered as mainshock in the ESHM20 declustered catalogue (Danciu
126 et al., 2021; 2022). Where available, the converted PGA values were replaced by the recorded ones from the post-1977 VRI
127 events dataset of Manea et al., (2022). We did not include any intensity measure which is related to the events identified as
128 foreshock, aftershock, or swarm events. Depending on the available data, the intensity values were translated to PGA using
129 the latest conversion equations proposed by Ardeleanu et al., (2020) for the VRI source and Caprio et al., (2015) for global
130 crustal as no local shallow models are available. A different conversion equation was used for VRI as the observed
131 macroseismic field presents unique features which are not seen for shallow seismicity, such as: an azimuthal asymmetric shape
132 due to the source properties (Marmureanu et al., 2016b; Craiu et al., 2023), different apparent attenuation patterns due to the
133 unique tectonic environment (e.g. Manea et al., 2022) and far-field strong site effects (Cioflan et al., 2022). The equation of
134 Ardeleanu et al., (2020) was selected as it is the most recent intensity to PGA conversion equations proposed for VRI and its
135 predictions agree with the ones from the previous studies, such as Vacareanu et al., (2015) and Marmureanu et al., (2011). The
136 distribution of the MSK to PGA conversions and their corresponding standard deviations up to X MSK-64 are presented in
137 *Figure S1*, which can be found in the electronic *Supplementary Materials*. Each IDP was translated into three PGA values, i.e

138 the mean IPE model and its standard deviation, to consider the variability of this conversion into the final results. The IDP was
 139 translated to PGA as it's simply less challenging and more efficient than converting all the PGA hazard curves to intensity.
 140 To align to the ESHM20 rock conditions, for which the time-averaged shear-wave velocity to 30 m depth (V_{s30}) is set to 800
 141 m/s, the ground-motion amplitudes were corrected for site effects considering amplification in each city by means of soil
 142 factors recommended in Eurocode 8 (Comité Européen de Normalisation (CEN), 2004, EC8) for crustal seismicity and the
 143 ones adjusted for Vrancea earthquakes proposed by Vacareanu et al., (2014). The EC8 site classes were gathered from Manea
 144 et al., (2022) and Coman et al., (2020) studies and are presented in Table 1. The use of observational intensity data to compare
 145 against hazard curves introduces additional layers of uncertainty. One must acknowledge the complex process of converting
 146 subjective intensity measures into objective ground acceleration values, given the uncertainty nature of intensity observations
 147 and the variability in the human experience of ground shaking (e.g. Rey et al., 2018). Furthermore, the determination of
 148 complete and reliable historical records for specific macroseismic intensity levels is equally challenging, presenting a
 149 considerable difficulty in aligning the past seismicity with probabilistic forecasts. We incorporated the full uncertainty
 150 variability within the PGA calculations by considering the uncertainty on the conversion from intensity to PGA, to evaluate
 151 how much these uncertainties impact the results of the hazard testing.
 152



153
 154 **Figure 3: The distribution of the selected intensity data points used for the ESHM20 hazard testing at the twelve cities, with a**
 155 **threshold above V MSK-64. The timeline and primary source information for the major earthquakes, which significantly affected**
 156 **Romanian territory, are presented in the upper side of the plot.**

157 4 Statistical Testing Procedure

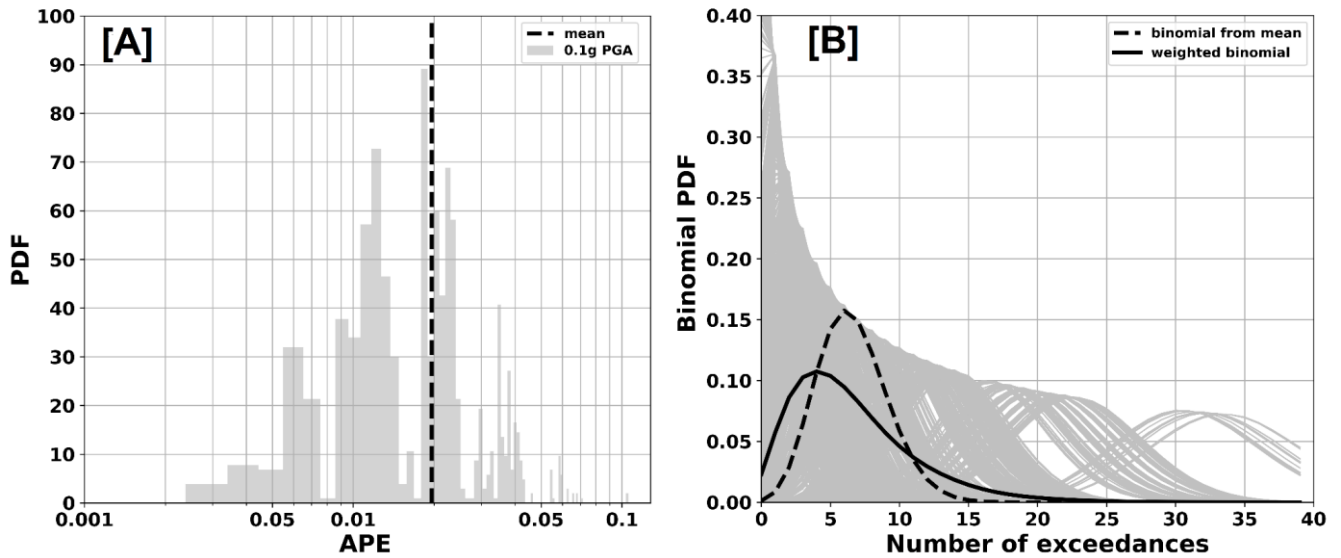
158 In the following section, we provide an overview of our methodology for evaluating the performance of the ESHM20 ground
159 shaking estimates by comparing them to instances of ground motion exceedances at twelve main cities in Romania. The
160 statistical testing relies upon comparing the actual occurrences of ground acceleration surpassing specific thresholds (0.1 and
161 0.2g PGA) with the ESHM20 estimates, by considering the associated uncertainties. The selected ground motion levels are of
162 relevance to PSHA in Romania, with 0.1g approximating the lower bound of damaging ground motions. First, we compile the
163 full dataset of ground shaking that includes both the recordings (where available) and the macroseismic observations converted
164 to PGA by considering uncertainties of the conversion process and the influence of site conditions. Next, we determine the
165 specific time period of this dataset and count the instances where the acceleration thresholds are surpassed to obtain the
166 distribution of the observed number of exceedances over the time period of completeness.

167 Subsequently, we follow closely the statistical testing approach proposed by Marzocchi and Jordan (2014, 2017, 2018), which
168 accounts for both the aleatory and the epistemic uncertainties of the hazard (Meleti et al., 2021; Stirling et al., 2023). The
169 above-mentioned methodology considers that the exceedance rate variability is well represented by a binomial distribution.
170 We forecast the anticipated number of exceeding occurrences for each logic-tree branch by using the proposed binomial
171 distribution (Stirling et al., 2023) and build the sum of all the weighted distributions by considering each branch weight to
172 evaluate the likelihood of observing the exact number of exceedances.

173 The variability of the 10000 random samples of the hazard curves for Bucharest, capital of Romania, is presented in *Figure*
174 *2B*, while the contribution of various logic tree branches to hazard at 0.1g PGA is illustrated in *Figure 4A*. It shows that the
175 mean hazard value doesn't explain the APEs asymmetric distribution. Thus, for this analysis we use the weighted binomial
176 distribution considering the APEs distribution of the entire ESHM20 logic tree branches. The variability of all the computed
177 binomials for the entire ensemble of the hazard curves are presented in *Figure 4B*, alongside the final weighted mean
178 considering the full distribution of the uncertainties and the resulting binomial retrieved from the statistical mean. The
179 distribution of the APEs reflects the contribution of various logic tree branches, and the differences between the two statistical
180 descriptors i.e., weighted mean versus statistical mean is evident in *Figure 4B*.

181

182



183

184

Figure 4: [A] Probability density functions computed for 0.1g PGA level versus annual probability of exceedance - APE. The vertical black line indicates the traditional hazard mean value. [B] The variability of the computed binomials for all the hazard ensembled curves (grey lines) is shown together with the final weighted mean curve considering the full distribution of the uncertainties, and the one computed from the commonly used mean hazard curve.

185

186

187

188

189

Based on the above-mentioned methodology, we perform point-based testing at each of the twelve cities using the following steps:

191

192

193

194

195

196

197

198

199

200

201

202

1. Estimate the time-period of available ground motion for each city in the compiled ground motion dataset (in terms of PGA corrected values for site effects).
2. Count observed exceedances of PGA at 0.1g and 0.2g levels for each city complete time window and calculate their corresponding standard deviations considering the uncertainties in the intensity to PGA conversions.
3. Calculate the predicted number of exceedances for each of the PGA thresholds considering every end-branch of the ESHM2022 logic tree (i.e., annual probability of exceedance \times total time-period)
4. Compute the weighted mean binomial distribution by combining all the binomial distributions applied to (3) considering the full distribution of the hazard uncertainties. Calculate the probability (*p-value*) that the observed number of exceedances could be drawn from the weighted mean binomial distribution.
5. Compute the *p-value* where there will be N observations or more than the observed number of exceedances from the weighted mean binomial distribution.

203 5 Statistical Testing Procedure: Results

204 The results of the statistical testing of ESHM20 at 0.1 and 0.2g PGA are illustrated in *Figures 5* and *6* for six cities (Focșani,
205 Brașov, Bucharest, Iași, Constanța, and Timișoara), while for the others (Bacău, Câmpulung, Cluj-Napoca, Craiova, Galați,
206 Sibiu) are given in *Figures S2 and S3* of the *Supplementary Materials*. These plots depict the histogram of the weighted mean
207 of ESHM20, the observed number of exceedances (i.e., black vertical line) and its one sigma variability (i.e., dashed vertical
208 lines). The total time of the observations is specified in each subplot for their respective city. As mentioned before, the average
209 time period of the observations of both ground shaking recordings and macroseismic data spans over 322 years for all the
210 cities, except the ones in the within the Carpathian region, such as: Sibiu and Cluj-Napoca, as well as Timișoara, the
211 westernmost city. For these cities, the time period is about 220 years. Overall, there is a consistent alignment of estimated
212 ground shaking hazard of ESHM20 with the observed data at 0.1g PGA level, as shown by *Figure 5*. Notably, cities located
213 along the northeast-southwest trajectory outside the Carpathians - such as Iași, Focșani, and Bucharest (see *Figure 5*) - show
214 a robust correlation with the ESHM20 PGA estimates. Of particular interest, it's the consistency of the ESHM20 with
215 observations for Focșani, the city found in the proximity of the Vrancea deep seismicity sources, the main seismogenic source
216 of the region. A slight shift from the ESHM20 prediction is observed for the capital city of Romania, i.e, Bucharest, where
217 more intensities over VII MSK-64 were recorded than predicted; this fact might reflect the impact of the way humans
218 experienced ground shaking within different typologies of buildings in megacities (Rogozea, 2016; Cioflan et al., 2016). Also,
219 such a shift might be attributed to the effect of different source and path features, such as directivity, or uncertainties in
220 correcting for site-effects. Furthermore, the values expected from ESHM20 are over the observed ones for cities along and in
221 the proximity to the Carpathian bend, e.g., Bacău, Brașov and Câmpulung, and might suggest that a local attenuation effect is
222 not currently captured or modelled using the ESHM20 scaled backbone logic tree for the Vrancea in-slab region (Weatherill
223 et al., 2020). The impact of different attenuation patterns due to the complex tectonic configuration was previously seen on
224 both human-felt and instrumental observations (e.g, Radulian et al., 2006; Ivan, 2007; Marmureanu et al., 2016b) and captured
225 within the recent region-specific ground motion models (GMMs; e.g. Vacareanu et al., 2015; Manea et al., 2022). The results
226 at the cities beyond the Carpathian Mountains (e.g., Sibiu, Cluj-Napoca, Timișoara) exhibit hazard predictions that reflect the
227 frequent crustal seismic activity as a significant attenuation behind the arc reduces VRI-related ground motion. It appears that
228 a longer and more comprehensive dataset may be required to accurately assess the distribution of ground shaking hazard levels.
229 For cities located in the far-field area of VRI and outside of the Carpathian arc (fore-arc region), such as Constanța and Craiova,
230 the computed hazard is slightly lower than the recorded data. The same feature can be seen from the 475 return-period PGA
231 map (see *Figure 1*), and it contrasts with the recorded ground motion field and pre-instrumental intensity data (e.g., Cioflan et
232 al., 2022). Manea et al. (2022) provide insights of the apparent attenuation of the ESHM20 ground motion model for the fore-
233 arc area and future adjustments of the ESHM20 are recommended to capture the ground motion characteristics within this
234 region of Romania. However, the estimates of ESHM20 at 0.1g PGA appear overall to be consistent to the data, given all the
235 uncertainties involved in this analysis. Similarly, for the 0.2 g PGA level, the results suggest a strong correlation in areas near

236 the VRI source (see *Figure 6* and *Figure S3*). Focșani experiences multiple instances of surpassing the 0.1g PGA level and the
237 observed exceedances are within the ESHM20 estimated binomial distribution. Nevertheless, for the remaining cities,
238 ESHM20 exceedances are slightly below observed exceedances in Bucharest and Iași, due to the influence of source/path
239 effects and/or uncertainties in correcting for site-effects. For the cities located along the Carpathian arc (Bacău, Brașov and
240 Câmpulung), the trend is reversed, with ESHM20 exceedances being higher than the observed ground shaking recurrences.
241 For the rest of the cities (Galați, Craiova, Timișoara, Sibiu, Conștanta, Cluj-Napoca), the ESHM20 estimates fit the
242 observations relatively well. The comparison between the observations and the weighted mean and the range of annual
243 probabilities of exceedance from ESHM20 hazard curves are consistent for the 0.1g PGA level. For the 0.2g PGA level, the
244 consistency is valid for the cities located in the proximity of the VRI.
245 The overall results are listed in Table 1 and the probability that the observed record could be drawn from the combined
246 distribution (*p-value*) is presented at each location as “P 0.1” and “P 0.2”. These results show that nine out of twelve locations
247 provide no evidence for poor performance of the ESHM20 for 0.1g PGA (poor performance - *p-value* < 0.05), while only at
248 one location the hazard doesn’t pass the test at 0.2g. Overall, the testing results suggest that there are no reasons to reject the
249 ESHM20 in Romania for 0.1 and 0.2g PGA.

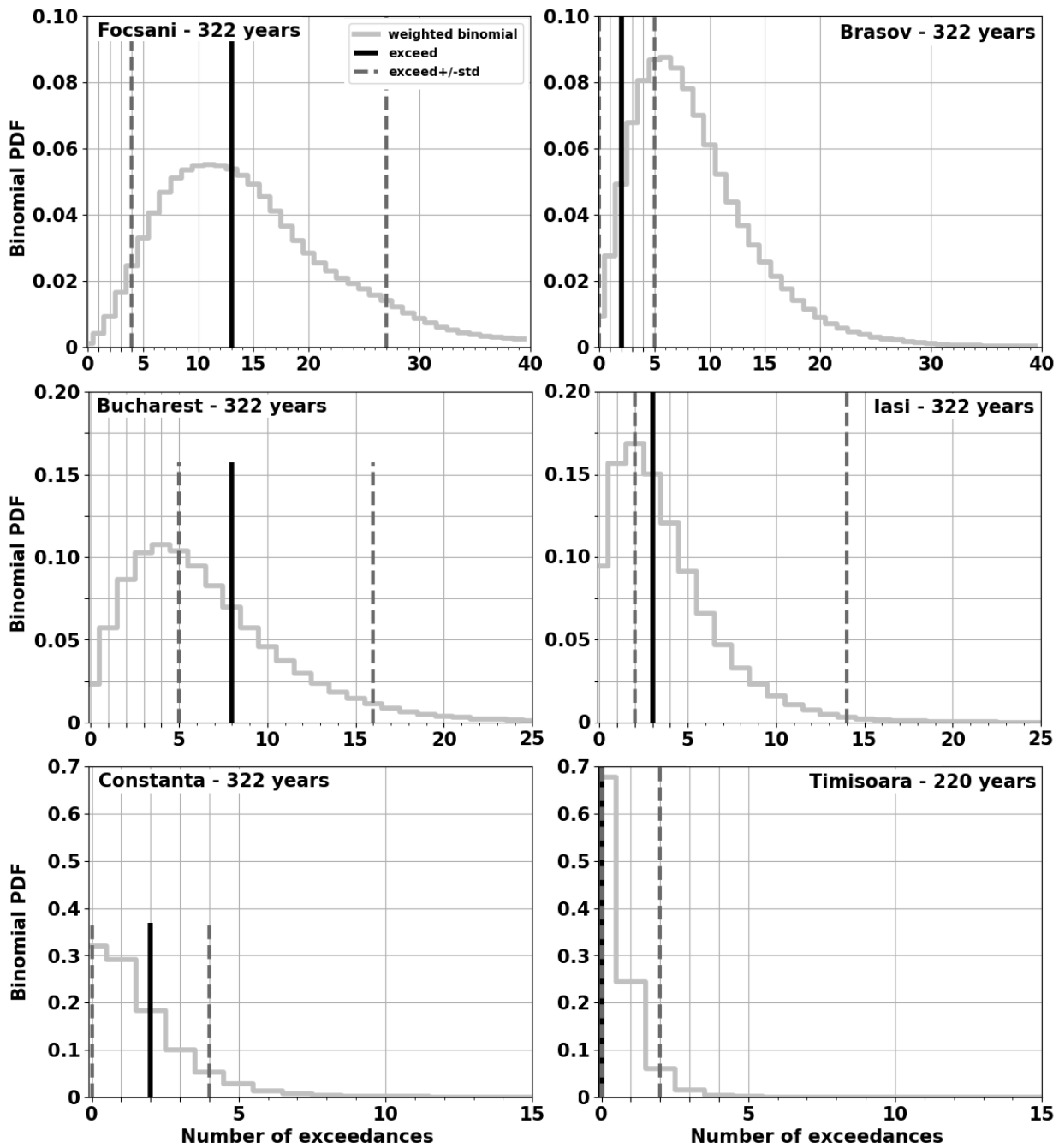
250 **6 Conclusions**

251 Evaluating the performance of seismic hazard models against recorded data, is an emerging research topic. In this study, we
252 evaluated the performance of the recent update of the ESHM20 (Danciu et al., 2021) in Romania. The compiled ground shaking
253 database combines strong motion records and macroseismic intensity data. The inclusion of the macroseismic intensity data,
254 allows expansion of the observational time period to over two to three hundred years, at the cost of increased uncertainties of
255 the ground motion estimates. The result of the statistical testing suggests that the ESHM20 is consistent with the observations
256 for two PGA levels, at the locations of the twelve cities selected across Romania. We found a strong consistency between the
257 weighted mean of ESHM20 and the exceedances of the observations for the cities (Focșani and Galați) located in the proximity
258 of the VRI source for both PGA levels i.e., 0.1g and 0.2g.

259 For cities located along the Carpathian arc (Bacău, Brașov and Câmpulung), the ESHM20 exceedances are above the recorded
260 ground motions and suggest that the along-arc attenuation effect (Manea et al., 2022) might not be captured or modelled in the
261 ESHM20 ground motion model (Weatherill et al., 2020). Furthermore, the testing results at cities located in the VRI far-field
262 area and outside of the Carpathian arc (Conștanta, Craiova), might suggest that the ground motion models used in ESHM20
263 attenuate too fast compared to the recorded PGA, as observed by Manea et al. (2022). For the Iași and Bucharest sites, located
264 along the NE-SW direction from the VRI source, the ESHM20 estimates appears to be below the recorded data at the 0.1g
265 PGA level and this feature become more prominent at 0.2 g; these differences might be attributed to: 1) source directivity
266 effects which are significant for major events occurring in Vrancea (Cioflan et al., 2022), 2) potential bias in the conversion
267 of the intensity to PGA, or 3) possible complex local site effects which might not been completely removed from the

268 observations. While informative conclusions could be drawn from evaluating the comparison at cities along and outside of the
269 Carpathian range, limited conclusions can be derived for locations in regions of low seismic hazard, such as Sibiu and Cluj-
270 Napoca, or Timișoara, in the western Romania. The seismic hazard of these regions is dominated by episodic clusters of small
271 to moderate shallow seismicity with regional effects, which are not well captured in the macroseismic data or the amount of
272 strong motion recordings. We acknowledge that even with a time period of two to three centuries, the observations remain
273 largely incomplete in time and space. The Romanian seismic network (Marmureanu et al., 2021) has evolved over time,
274 however limited ground motion data is available due to lack of significant earthquakes occurring in the recent decade or so.
275 Uncertainties associated with the ground motion dataset are increasing with the conversion of the macroseismic data, as
276 illustrated in the results given in *Figures 5* and *6*. Moreover, the statistical testing is limited in scope given all the uncertainties
277 are associated also with the distribution of the hazard results, configuration of the logic tree, sampling technique, and/or use
278 of a certain distribution i.e., binomial or log-normal. All these factors are contributing to the overall stability of the statistical
279 testing.

280 In conclusion, our analysis suggests that observed exceedance rates for these two PGA levels, i.e., 0.1g and 0.2g, are consistent
281 with ESHM20 estimates. These results must be interpreted with caution given the above-mentioned limitations in time and
282 spatial coverage of the observations, both the ground shakings and the macroseismic intensity dataset.



283

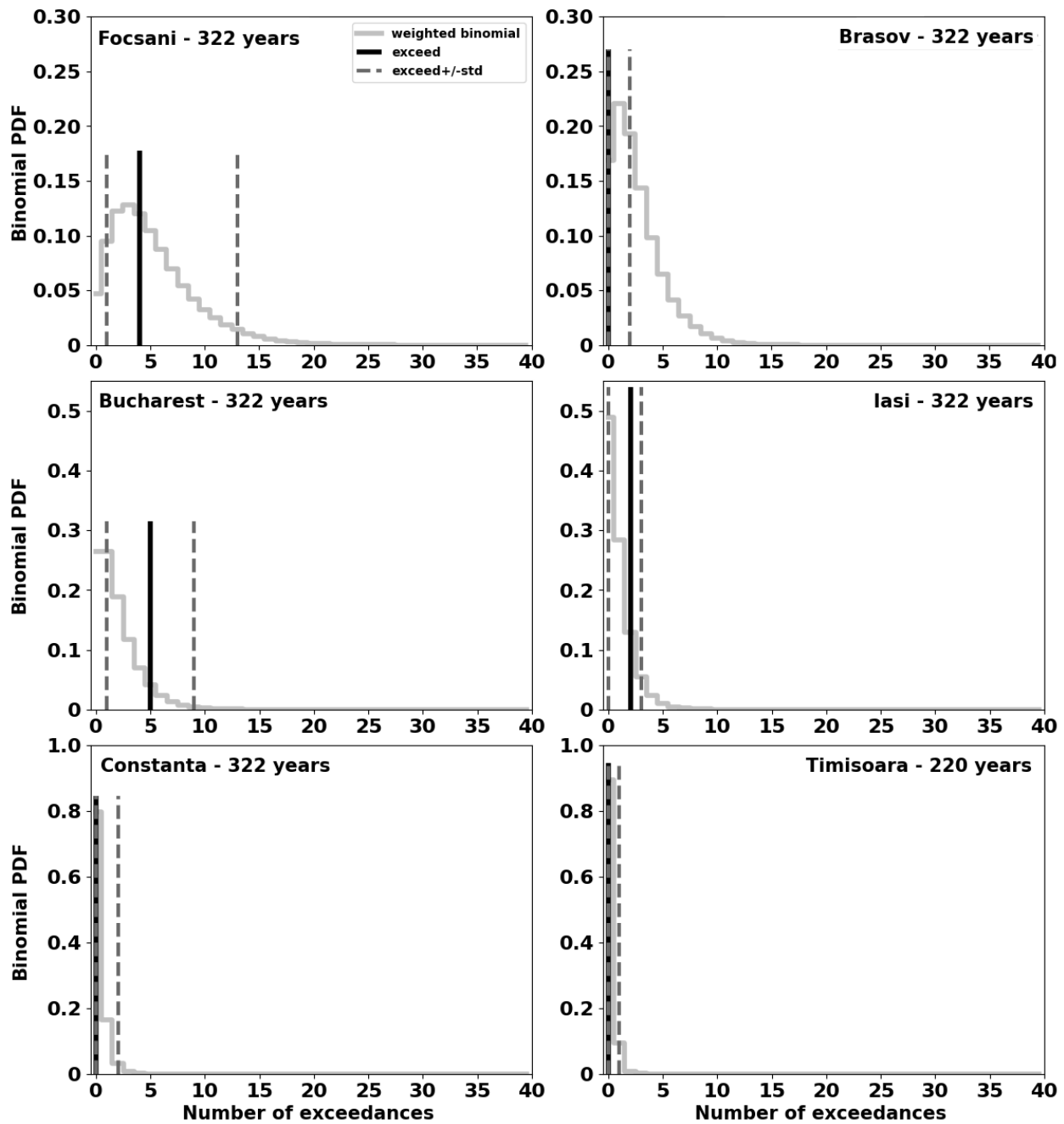
284

285

286

287

Figure 5. Consistency test results of ESHM20 with the observed PGA values at 0.1 g for each of six cities: Focșani, Brașov, Bucharest, Iași, Constanța, and Timișoara. The histogram depicts the ESHM20 weighted mean, the observed number of exceedances over the time window of completeness is given as the black vertical line and its one sigma variability i.e., dashed vertical lines; the total completeness time is specified in each subplot for their respective city.



288

289

290

291

292

Figure 6. Consistency test results of ESHM20 with the observed PGA values at 0.2 g for six representative cities. The histogram depicts the ESHM20 weighted mean, the observed number of exceedances over the time window of completeness is given as the black vertical line and its one sigma variability i.e., dashed vertical lines; the total completeness time is specified in each subplot for their respective city.

293
294

Table 1. Observed and the ESHM 2020 predicted exceedances for 0.1 and 0.2g PGA at twelve Romanian cities.

City	T	SC	N 0.1	Rate 0.1	APE 0.1	P 0.1	P> 0.1	N 0.2	Rate 0.2	APE 0.2	P 0.2	P> 0.2
Bacău	322	C	4	0.01242	0.01235	0.06551	0.88613	2	0.00621	0.00619	0.12691	1.00000
Braşov	322	B	2	0.00621	0.00619	0.04927	0.96333	1	0.00311	0.00310	0.16854	1.00000
Bucharest	322	C	8	0.02484	0.02454	0.06947	0.34191	5	0.01553	0.01541	0.04063	0.09541
Câmpulung	322	B	1	0.00311	0.00310	0.04146	0.98512	1	0.00311	0.00310	0.21444	1.00000
Cluj-Napoca	284	B	1	0.00352	0.00351	0.13002	0.14835	1	0.00352	0.00351	0.95985	1.00000
Constanţa	322	C	2	0.00621	0.00619	0.18241	0.38990	1	0.00311	0.00310	0.79675	1.00000
Craiova	322	C	3	0.00932	0.00927	0.08392	0.16519	1	0.00311	0.00310	0.82129	1.00000
Focşani	322	C	13	0.04037	0.03957	0.05461	0.55554	4	0.01242	0.01235	0.11991	0.60844
Galaţi	322	B	4	0.01242	0.01235	0.09490	0.78712	1	0.00311	0.00310	0.24510	0.77985
Iaşi	322	B	3	0.00932	0.00927	0.15007	0.58011	2	0.00621	0.00619	0.12878	0.22567
Sibiu	250	B	1	0.00400	0.00399	0.30161	0.48469	1	0.00400	0.00399	0.87168	1.00000
Timişoara	220	B	1	0.00455	0.00454	0.67819	1.00000	1	0.00455	0.00454	0.89580	1.00000

295

296 Where:

297 T = time window of completeness [years];

298 SC = EC8 site class (CEN, 2004);

299 N 0.1 (N 0.2) = number of observed exceedances in T for 0.1 (0.2) g PGA;

300 Rate 0.1 (Rate 0.2) = observed annual rate of exceedance for 0.1 (0.2) g PGA;

301 APE 0.1 (APE 0.2) = Annual probability of exceedance for 0.1g - calculated from observed rate;

302 P 0.1 (P0.2) = *P-value* that the observed number of exceedances within T could be drawn from ESHM20 for 0.1 (0.2) g;

303 P>0.1 (P>0.2) = *P-value* where there will be N observations or more than the observed number of exceedances within T could

304 be drawn from ESHM20 for 0.1 (0.2) g PGA

305 **Supplementary Material**

306 The electronic Supplement contains additional plots of the distribution of the MSK-64 Intensity to PGA conversions for the
307 two selected equations and the testing results for six cities and a summary plot of the results at all the locations.

308 **Data availability**

309 The collected intensity data can be made available by the authors only upon request as this study was done within an ongoing
310 project. The OpenQuake Engine input files and running scripts for ESHM20 can be downloaded from:
311 <https://gitlab.seismo.ethz.ch/efehr>.

312 **Author contributions**

313 EFM and LD designed the framework of the work. EFM, LD and MG developed the codes and performed the testing analysis.
314 CCO and DTD collected and harmonised the intensity data. EM and LD designed and wrote the paper with contributions from
315 the other co-authors.

316

317 **Competing interests**

318 The authors declare that they have no conflict of interests.

319

320 **Acknowledgments**

321 This study was carried out within the National Research Program SOL4RISC Grant No. 24N/2023, project no. PN23360202.
322 The second author received support and resources from Geo-INQUIRE Project, Grant agreement ID: 1010585182,
323 DOI10.3030/101058518. The seismic hazard calculations at the selected locations were performed using the OpenQuake
324 Engine version 3.14 (DOI 10.13117/openquake.engine, last accessed 01.06.2023). The software suite ArcGis
325 (www.esri.com/software/arcgis, last accessed 01.03.2023) was used for mapping and all the plots were done with Python using
326 open-source libraries. Part of the python investigation codes were developed within the New Zealand National Seismic Hazard
327 Model 2022 Revision Project (contract 2020-BD101).

328

329 **References**

- 330 Allen, T.I., Ghasemi, H, and Griffin, J.D.: Exploring Australian hazard map exceedance using an Atlas of historical
331 ShakeMaps. *Earthquake Spectra*, 39(2), 985-1006, doi:10.1177/87552930231151977, 2023.
- 332 Ardeleanu, L., Leydecker, G., Bonjer, K.-P., Busche, H., Kaiser, D., and Schmitt, T.: Probabilistic seismic hazard map for
333 Romania as a basis for a new building code, *Nat. Hazards Earth Syst. Sci.*, 5, 679–684, doi: 10.5194/nhess-5-679-2005.
- 334 Atanasiu, I.: *Cutremurele de pamant din Romania*, Ed. Academiei Romane, 196 p, Bucharest, 1961.
- 335 Caprio, M., Tarigan, B., Worden, C. B., Wiemer, S., & Wald, D. J.: Ground Motion to Intensity Conversion Equations
336 (GMICES): A Global Relationship and Evaluation of Regional Dependency. *Bulletin of the Seismological Society of America*,
337 105 (3): 1476–1490. doi: <https://doi.org/10.1785/0120140286>, 2015.
- 338 Cioflan, C. O., Manea, E. F., & Apostol, B. F. (2022). Insights from neo-deterministic seismic hazard analyses in Romania. In
339 *Earthquakes and sustainable infrastructure*, p. 415-432, Elsevier, <https://doi.org/10.1016/B978-0-12-823503-4.00013-0>, 2022.
- 340 Cioflan, C.O., Toma-Danila, D., and Manea, E.F.: Seismic Loss Estimates for Scenarios of the 1940 Vrancea Earthquake. In:
341 Vacareanu, R., Ionescu, C. (eds) *The 1940 Vrancea Earthquake. Issues, Insights and Lessons Learnt*. Springer Natural Hazards.
342 Springer, Cham. https://doi.org/10.1007/978-3-319-29844-3_30, 2016.
- 343 Coman, A., Manea, E. F., Cioflan, C. O., & Radulian, M.: Interpreting the fundamental frequency of resonance for
344 Transylvanian Basin. *Romanian Journal of Physics*, 65, 809, 2020.
- 345 Comité Européen de Normalisation (CEN): Eurocode 8, design of structures for earthquake resistance—Part 1: General rules,
346 seismic actions and rules for buildings. European Standard NF EN 1998-1. Brussels: CEN, 2004.
- 347 Constantin A. P., Pantea A., Stoica R.: Vrancea (Romania) Subcrustal Earthquakes: Historical Sources and Macroseismic
348 Intensity Assessment, *Romanian Journal of Physics*, 56, 5-6, p. 813 – 826, 2011.
- 349 Constantin, A. P., Moldovan, I. A., Craiu, A., Radulian, M., and Ionescu, C.: Macroseismic intensity investigation of the
350 November 2014, M=5.7, Vrancea (Romania) crustal earthquake, *Annals of Geophysics*, 59, 5, doi:10.4401/ag-6998, 2016.
- 351 Constantin, A., Manea, L., Diaconescu, M., & Moldovan, I.: Intensity and macroseismic maps of the latest moderate sized
352 Vrancea earthquakes. *Romanian Reports in Physics*, 75, 702, 2023.
- 353 Constantin, A.P., Pantea, A. Macroseismic field of the October 27, 2004 Vrancea (Romania) moderate subcrustal earthquake.
354 *J Seismol* 17, 1149–1156, <https://doi.org/10.1007/s10950-013-9383-2>, 2013.
- 355 Craiu, A., Ferrand, T. P., Manea, E. F., Vrijmoed, J. C., and Mărmureanu, A.: A switch from horizontal compression to vertical
356 extension in the Vrancea slab explained by the volume reduction of serpentine dehydration. *Sci Rep* 12, 22320,
357 <https://doi.org/10.1038/s41598-022-26260-5>, 2022.
- 358 Craiu, A., Craiu, M., Mihai, M., Manea, E. F., & Marmureanu, A. (2023). Vrancea intermediate-depth focal mechanism
359 catalog: a useful instrument for local and regional stress field estimation. *Acta Geophysica*, 71(1), 29-52.

360 Danciu, L., Nandan, S., Reyes, C., Basili, R., Weatherill, G., Beauval, C., Rovida A., Vilanova, S., Sesetyan, K., Bard, P-
361 Y., Cotton, F., Wiemer, S., and Giardini, D.: The 2020 update of the European Seismic Hazard Model: Model
362 Overview. EFER Technical Report 001, v1.0.0, <https://doi.org/10.12686/a15>, 2021.

363 Danciu, L., Weatherill, G., Rovida, A., Basili, R., Bard, P.Y., Beauval, C., Nandan, S., Pagani, M., Crowley, H., Sesetyan, K.,
364 Villanova, S., Reyes, C., Marti, M., Cotton, F., Wiemer, S., and Giardini, D.: The 2020 European Seismic Hazard Model:
365 Milestones and Lessons Learned. In: Vacareanu, R., Ionescu, C. (eds) *Progresses in European Earthquake Engineering and*
366 *Seismology*. ECEES 2022. Springer Proceedings in Earth and Environmental Sciences. Springer, Cham.
367 https://doi.org/10.1007/978-3-031-15104-0_1, 2022.

368 Danciu, L., Giardini, D., Weatherill, G., Basili, R., Nandan, S., Rovida, A., Beauval, C., Bard, P.-Y., Pagani, M., Reyes, C.
369 G., Sesetyan, K., Vilanova, S., Cotton, F., and Wiemer, S.: The 2020 European Seismic Hazard Model: Overview and Results,
370 EGUSphere [preprint], <https://doi.org/10.5194/egusphere-2023-3062>, 2024. Ferrand, T.P., Manea, E.F.: Dehydration-induced
371 earthquakes identified in a subducted oceanic slab beneath Vrancea, Romania. *Sci Rep* 11, 10315.
372 <https://doi.org/10.1038/s41598-021-89601-w>, 2021.

373 Gerstenberger, Matthew C., Warner Marzocchi, Trevor Allen, Marco Pagani, Janice Adams, Laurentiu Danciu, Edward H.
374 Field et al.: Probabilistic seismic hazard analysis at regional and national scales: State of the art and future challenges. *Reviews*
375 *of Geophysics* 58, no. 2 (2020): e2019RG000653.

376 Giardini, D., Wössner, J., and Danciu, L.: Mapping Europe's seismic hazard. *Eos, Transactions American Geophysical Union*,
377 95, 29, 261-262, <https://doi.org/10.1002/2014EO290001>, 2014.

378 Hanks, T. C., Beroza, G. C., & Toda, S.: Have recent earthquakes exposed flaws in or misunderstandings of probabilistic
379 seismic hazard analysis?. *Seismological Research Letters*, 83(5), 759-764, doi: <https://doi.org/10.1785/0220120043>, 2012.

380 Iervolino I., Chioccarelli E., Cito P.: Testing three seismic hazard models for Italy via multi-site observations. *PLoS ONE*
381 18(4): e0284909, <https://doi.org/10.1371/journal.pone.0284909>, 2023.

382 Ivan, M.: Attenuation of P and pP waves in Vrancea area–Romania. *Journal of seismology*, 11(1), 73-85,
383 <https://doi.org/10.1007/s10950-006-9038-7>, 2007.

384 Kronrod, T., Radulian, M., Panza, G., Popa, M., Paskaleva, I., Radovanovich, S., Gribovski, K., Sandu, I., and Pekevski, L.:
385 Integrated transnational macroseismic data set for the strongest earthquakes of Vrancea (Romania), *Tectonophysics*, 590, 1-
386 23, doi: 10.1016/j.tecto.2013.01.019, 2013.

387 Mak, S., Schorlemmer, D.: A Comparison between the Forecast by the United States National Seismic Hazard Maps with
388 Recent Ground-Motion Records. *Bulletin of the Seismological Society of America*; 106 (4): 1817–1831. doi:
389 <https://doi.org/10.1785/0120150323>, 2016.

390 Manea, E. F., Predoiu, A., Cioflan, C. O., & Diaconescu, M.: Interpretation of resonance fundamental frequency for Moldavian
391 and Scythian platforms. *Romanian Reports in Physics*, 71, 709, 2019.

392 Manea, E.F., Cioflan, C. O., and Danciu, L.: Ground-motion models for Vrancea intermediate-depth earthquakes. *Earthquake*
393 *Spectra*, 38, 1, 407-431, doi:10.1177/87552930211032985, 2022.

394 Marmureanu, G., Cioflan, C.O. and Marmureanu, A.: Intensity seismic hazard map of Romania by probabilistic and (neo)
395 deterministic approaches, linear and nonlinear analyses, *Rom. Rep. Phys.*, 63(1), 226-239, 2011.

396 Marmureanu, G., Cioflan, C.O., Marmureanu, A., and Manea, E.F.: Main Characteristics of November 10, 1940 Strong
397 Vrancea Earthquake in Seismological and Physics of Earthquake Terms. In: Vacareanu, R., Ionescu, C. (eds) *The 1940 Vrancea*
398 *Earthquake. Issues, Insights and Lessons Learnt*. Springer Natural Hazards. Springer, Cham. [https://doi.org/10.1007/978-3-](https://doi.org/10.1007/978-3-319-29844-3_5)
399 [319-29844-3_5](https://doi.org/10.1007/978-3-319-29844-3_5), 2016b.

400 Marmureanu, G., Marmureanu, A., Manea, E.F., Toma-Danila, D., and Vlad, M.: Can we still use classic seismic hazard
401 analysis for strong and deep Vrancea earthquakes. *Romanian Reports in Physics*, 61(3–4), 728-738, 2016a.

402 Marmureanu, G., Manea, E. F., Cioflan, C. O., Marmureanu, A., & Toma-Danila, D.: Spectral response features used in last
403 IAEA stress test to NPP Cernavoda (ROMANIA) by considering strong nonlinear behaviour of site soils. *Romanian Journal*
404 *of Physics*, 62, 822, 2017.

405 Marmureanu, G., Vacareanu, R., Cioflan, C.O., Ionescu, C., and Toma-Danila, D.: Historical Earthquakes: New Intensity Data
406 Points Using Complementary Data from Churches and Monasteries (chapter). *Seismic Hazard and Risk Assessment. Updated*
407 *Overview with Emphasis on Romania*. Ed: Vacareanu R., Ionescu C., Springer Natural Hazards, Springer International
408 Publishing, doi: 10.1007/978-3-319-74724-8_7, 2018.

409 Mărmureanu, A., Ionescu, C., Grecu, B., Toma-Danila, D., Tiganescu, A., Neagoe, C., ... & Ilieș, I.: From national to
410 transnational seismic monitoring products and services in the Republic of Bulgaria, Republic of Moldova, Romania, and
411 Ukraine. *Seismological Society of America*, 92(3), 1685-1703, 2021.

412 Marzocchi, W., and Jordan, T. H.: Experimental concepts for testing probabilistic earthquake forecasting and seismic hazard
413 models. *Geophysical Journal International*, 215, 2, 780-798, <https://doi.org/10.1093/gji/ggy276>, 2018.

414 Marzocchi, W., and Jordan, T.H.: A unified probabilistic framework for seismic hazard analysis, *Bull. Seismol. Soc. Am.*,
415 107(6), 2738-2744, <https://doi.org/10.1785/0120170008>, 2017.

416 Marzocchi, W., and Jordan, T.H.: Testing for ontological errors in probabilistic forecasting models of natural systems, *Proc.*
417 *Natl. Acad. Sci.*, 111(33), 11973- 11978, <https://doi.org/10.1073/pnas.1410183111>, 2014.

418 Medvedev, S.V., Sponheuer, W. and Karnik, V.: Seismic intensity scale version MSK 1964, *Publ. Inst. Geodynamik*, 48, Jena
419 48, 1967.

420 Meletti, C., Marzocchi, W., D'Amico, V., and Lanzano, G., The new Italian seismic hazard model (MPS19). *Annals of*
421 *Geophysics* 64(1), DOI:10.4401/ag-8579, 2021.

422 Mousavi, S.M., Beroza, G.C.: Evaluating the 2016 One-Year Seismic Hazard Model for the Central and Eastern United States
423 Using Instrumental Ground-Motion Data. *Seismological Research Letters* 89 (3): 1185–1196. doi:
424 <https://doi.org/10.1785/0220170226>, 2018.

425 Musson, R.M.W., Grünthal, G., and Stucchi, M.: The comparison of macroseismic intensity scales. *Journal of Seismology*, 14,
426 413-428, <https://doi.org/10.1007/s10950-009-9172-0>, 2010.

427 Oncescu, M.C., Marza, V.I., Rizescu, M., Popa, M.: The Romanian earthquake catalogue between 984–1997. In “Vrancea
428 Earthquakes: Tectonics, Hazard and Risk Mitigation: Contributions from the First International Workshop on Vrancea
429 Earthquakes”, Bucharest, Romania, November 1–4, 1997, pp. 43-47. https://doi.org/10.1007/978-94-011-4748-4_4, 1999.

430 Pagani, M., Monelli, D., Weatherill, G., Danciu, L., Crowley, H., Silva, V., ... & Simionato, M.: OpenQuake engine: An open
431 hazard (and risk) software for the global earthquake model. *Seismological Research Letters*, 85(3), 692-702, doi:
432 <https://doi.org/10.1785/0220130087>, 2014.

433 Radu, C.: Catalogue of Strong Earthquakes Originated on the Romanian Teritmt T, Part I: Before 1901. In *Seismological
434 Researches on the Earthquake of March 4, 1977*, Monograph (eds. Cornea, I. and Radu, C.) (Central Institute of Physics,
435 Bucharest), 1979.

436 Radulian, M., Panza, G. F., Popa, M., & Grecu, B.: Seismic wave attenuation for Vrancea events revisited. *Journal of
437 Earthquake Engineering*, 10(03), 411-427, <https://doi.org/10.1080/13632460609350603>, 2006.

438 Rey, J., Beauval, C., and Douglas, J.: Do French macroseismic intensity observations agree with expectations from the
439 European Seismic Hazard Model 2013?, *Journal of Seismology*, 22, 589-604, <https://doi.org/10.1007/s10950-017-9724-7>,
440 2018.

441 Rogozea M., Marmureanu G., Radulian M., Toma D.: Reevaluation of the macroseismic effects of the 23 January 1838
442 Vrancea earthquake. *Romanian Reports in Physics*, 66(2):520-538, 2014.

443 Rogozea M.: *Impactul cutremurelor majore din România: trecut, prezent și viitor*. Editura Electra, București, 2016.

444 Rovida A., Albini P., Locati M., Antonucci A.: Insights into Preinstrumental Earthquake Data and Catalogs in Europe.
445 *Seismological Research Letters*, 91(5), 2546–2553, <https://doi.org/10.1785/0220200058>, 2020.

446 Salditch, L., Gallahue, M. M., Lucas, M. C., Neely, J. S., Hough, S. E., and Stein, S.: California Historical Intensity Mapping
447 Project (CHIMP): A consistently reinterpreted dataset of seismic intensities for the past 162 yr and implications for seismic
448 hazard maps. *Seismological Research Letters*, 91(5), 2631-2650, doi: <https://doi.org/10.1785/0220200065>, 2020.

449 Shebalin N.V., Karnik V., Hadzievski D.: UNDP-Unesco Survey of the Seismicity of Balkan Region. *Catalogue of earthquakes
450 of the Balkan region*. Printing Office of the University Kiril and Metodij, Skopje, 599p., 1974.

451 Sibson, R.: A Brief Description of Natural Neighbor Interpolation. In: Barnett, V., Ed., *Interpreting Multivariate Data*, John
452 Wiley & Sons, New York, 21-36, 1981.

453 Sokolov, V. Y., Wenzel, F., and Mohindra, R.: Probabilistic seismic hazard assessment for Romania and sensitivity analysis:
454 a case of joint consideration of intermediate-depth (Vrancea) and shallow (crustal) seismicity, *Soil Dynamics and Earthquake
455 Engineering*, 29(2), 364-381. <https://doi.org/10.1016/j.soildyn.2008.04.004>, 2009.

456 Sokolov, V., Bonjer, K. P., Wenzel, F., Grecu, B., and Radulian, M.: Ground-motion prediction equations for the intermediate
457 depth Vrancea (Romania) earthquakes. *Bull Earthquake Eng* 6, 367–388 <https://doi.org/10.1007/s10518-008-9065-6>, 2008.

458 Stirling, M., Manea, E., Gerstenberger, M., & Bora, S.: Testing and Evaluation of the New Zealand National Seismic Hazard
459 Model 2022. *Bulletin of the Seismological Society of America*, doi: <https://doi.org/10.1785/0120230108>, 2023.

460 Stirling, M.W., and Gerstenberger, M.C.: Ground motion-based testing of seismic hazard models in New Zealand. *Bulletin of*
461 *the Seismological Society of America*, 100(4): 1407-1414; doi: 10.1785/0120090336, 2010.

462 Tasan, H., Beauval, C., Helmstetter, A., Sandikkaya, A., & Guéguen, P: Testing probabilistic seismic hazard estimates against
463 accelerometric data in two countries: France and Turkey. *Geophysical Journal International*, 198(3), 1554-1571. doi:
464 <https://doi.org/10.1093/gji/ggu191>, 2014.

465 Vacareanu, R., Iancovici, M., Neagu, C., and Pavel, F.: Macroseismic intensity prediction equations for Vrancea intermediate-
466 depth seismic source, *Natural Hazards*, 79(3), 2005-2031, <https://doi.org/10.1007/s11069-015-1944-y>, 2015.

467 Vacareanu, R., Marmureanu, G., Pavel, F., Neagu, C., Cioflan, C. O., and Aldea, A.: Analysis of soil factor S using strong
468 ground motions from Vrancea subcrustal seismic source. *Rom Rep Phys*, 66(3), 893-906, 2014.

469 Vanneste, K., Stein, S., Camelbeeck, T., and Vleminckx, B.: Insights into earthquake hazard map performance from shaking
470 history simulations. *Scientific reports*, 8(1), 1855, <https://doi.org/10.1038/s41598-018-20214-6> , 2018.

471 Weatherill, G., Kotha, S. R., & Cotton, F.: A regionally-adaptable “scaled backbone” ground motion logic tree for shallow
472 seismicity in Europe: application to the 2020 European seismic hazard model. *Bulletin of Earthquake Engineering*, 18(11),
473 5087-5117, <https://doi.org/10.1007/s10518-020-00899-9>, 2020.

474 Weatherill, G., Kotha, S. R., Danciu, L., Vilanova, S., and Cotton, F.: Modelling seismic ground motion and its uncertainty in
475 different tectonic contexts: Challenges and application to the 2020 European Seismic Hazard Model (ESHM20). *Natural*
476 *Hazards and Earth System Sciences*, Preprint nhess-2023-124, 1-66, <https://doi.org/10.5194/nhess-2023-124>, 2023.